Received: 20 October 2021 | Revised: 6 January 2022 | Accepted: 15 January 2022

DOI: 10.1002/cnm.3572

BASIC RESEARCH

WILEY

A numerical study on the safety belt-to-pelvis interaction

Hosein Naseri | **Johan Iraeus** | **Håkan Johansson**

Mechanics and Maritime Sciences, Chalmers University of Technology, Gothenburg, Sweden

Correspondence
Hosein Naseri, Mechanics and Maritime Sciences, Chalmers University of Technology, Gothenburg, Sweden.
Email: hosein.naseri@chalmers.se

Present address
Hosein Naseri, Chalmers University of Technology, Gothenburg, Sweden

Funding information
European Union's Horizon 2020 Research and Innovation Program, Grant/Award Number: 768947; Vetenskapsrådet, Grant/Award Number: 621-2013-3909

Abstract

The slide of the lap belt over the iliac crest of the pelvis during vehicle frontal crashes can substantially increase the risk of some occupant injuries. A multitude of factors, related to occupants or the design of belt, are associated with this phenomenon. This study investigates safety belt-to-pelvis interaction and identifies the most influential parameters. It also explores how initial lap belt position influences the interaction between lap belt and pelvis. A finite element model of the interaction between lap belt with pelvis through a soft tissue part was created. Belt angle, belt force, belt loading rate and belt-to-body friction as belt design parameters, and pelvis angle, constitute parameters of soft tissue, and soft tissue-to-pelvis friction as occupant parameters were inspected. For the soft tissue part, subcutaneous adipose tissue with different thicknesses was created and the effect initial lap belt position may have on lap belt-to-pelvis interaction was investigated. The influential parameters have been identified as: the belt angle and belt force as belt design parameters and the pelvis angle and compressibility of soft tissue as occupant parameters. The risk for the slide of lap belt over the iliac crest of the pelvis was predicted higher as the initial lap belt positions goes superior to the pelvis. Of different submarining parameters, the lap belt angle represents the most influential one. The lap belt-to-pelvis interaction is influenced by the thickness of subcutaneous adipose tissue between lap belt and pelvis indicating a higher risk for obese occupants.

KEYWORDS

adipose tissue, human body models, lap belt-to-pelvis interaction, obesity, submarining

1 | INTRODUCTION

Three point seatbelts are known to be very effective in mitigating injuries in vehicle crashes.[1] In a vehicle crash, 3-point seatbelts prevent the body impacting interior structure by restraining the moving body at the pelvis, chest, and shoulders. However, improper seatbelt fit, and in particular the fit of the lap belt, might lead to the belt sliding over the anterior superior iliac spines (ASIS) during a frontal crash. This can cause abdominal injuries if the crash energy is sufficiently high. This scenario is referred to as submarining.[2] A wide range of different factors may affect the proper functionality of seatbelts including occupant characteristics, safety system design or crash-related parameters. Obesity,

for example, is one parameter that alters the proper fit of seatbelts and is associated with the increased risk of injury.[3–7] Obesity is most commonly defined by a person's Body Mass Index (BMI). BMI is calculated by dividing a person's body mass (in kilograms) by the square of their stature (in metres). The American Obesity Association defines a person obese if he or she has a BMI greater than 30 kg/m^2. Obesity introduces slack between the seatbelt and the underlying bony structure, because of a thicker layer of subcutaneous adipose tissue, which reduces seatbelt functionality. A static measurement of belt fit was conducted in literature.[3,4,8,9] Particularly, how the lap belt position is altered by obesity was investigated. Obesity moved the initial lap belt position further anterior-superior to the ASIS. This has been mentioned as one reason that exposes obese occupants to a higher risk of submarining, although the precise mechanism that gives rise to the higher risk of submarining has not been explored.

Towards understanding submarining mechanism, several studies[10–12] have investigated the lap belt-to-pelvis interaction by conducting lap belt pulling tests on post-mortem human subjects (PMHSs) fixed on a rigid sled. Lap belt was pulled with different forces, rates and angles at few belt positions. Their aim was to provide reproducible PMHS data in submarining test configuration for computational models such as human body models (HBMs) for vehicle safety. The Global Human Body Models Consortium (GHBMC)[13] and total human model for safety (THUMS)[14,15] are two examples of finite element HBMs (FEHBMs) extensively used for studying occupant kinematics and injury mechanisms. The previous studies[10–12] on lap belt-to-pelvis interaction used a few seat and belt configurations, with PMHSs mainly matching 50th percentile females and males. These tests are valuable for evaluating the biofidelity of FEHBMs. However, the variation in occupant and vehicle design parameters in these studies was quite limited. A more comprehensive investigation is required to understand the mechanism of lap belt-to-pelvis interaction to subsequently improve FEHBM biofidelity in particular for obese occupants. It is worth mentioning that most FEHBMs have been initially developed to study the overall occupant' responses in severe crashes and loads on the bony structures, not to specially study the details of belt-body interaction. For example, the biofidelity of the GHBMC model in reproducing submarining showed that the GHBMC model was not to able replicate the slide of belt over the pelvis.[16] Additionally, for the THUMS model, its abdominal region response was calibrated against two tests: a high-speed seatbelt loading[17] test and an anterior bar impact test,[18] both measuring the aggregate response of the abdomen, making them unsuitable for characterising belt-to-pelvis interaction.

This study aimed to conduct a comprehensive computational analysis of the lap belt-to-pelvis interaction to identify the main influential seatbelt design and occupant parameters. Especially, it aimed to ascertain what effect the thickness of subcutaneous adipose tissue[19] and initial lap belt position, may have on lap belt-to-pelvis interaction. The findings of this study can be used to indicate the effect of obesity on the belt to pelvis interaction, as well as be used as a guideline in the biofidelity development of FEHBMs.

2 | METHODS

Lap belt-to-pelvis interaction and possible influencing parameters, have been described in this section. A finite element pelvis submodel developed in a previous study[20] was employed to study lap belt-to-pelvis interaction. The parameter study was conducted in two steps: an individual parameter study and a full parameter variation investigation. In the individual parameter study, one parameter at the time was varied whereby parameters that have major effect on lap belt-to-pelvis interaction were selected. Then, a full variation matrix of these selected parameters was studied in the second step. All simulations were conducted in LS-Dyna (LSTC, Livermore, CA).

2.1 | The FE pelvis submodel

The interaction between the lap belt and the pelvis is regarded as a local phenomenon since the main deformation occurs within rather soft tissue.[20] Therefore, the FE pelvis submodel which has been inspired by preliminary simulations using the SAFER HBM v9,[21,22] features only soft tissue (skin and subcutaneous adipose tissue), abdomen and the iliac crest of the pelvis as well as the interaction with the lap belt, Figure 1. The same material models and material parameters as for SAFER HBM v9 were selected for the FE pelvis submodel, except for adipose tissue that the material model developed in a previous work[23] was selected. The effect of disregarded neighbouring parts has been accounted for in boundary conditions as follows. The pelvis has been clamped in the FE pelvis submodel. The posterior side of the abdomen has also been fixed to resemble the interaction with the spinal column. In physical tests, the soft tissue deforms sharply under the lap belt load, thus, the effect of the imposed deformation on the tissue behaviour at a short distance from the belt is negligible.

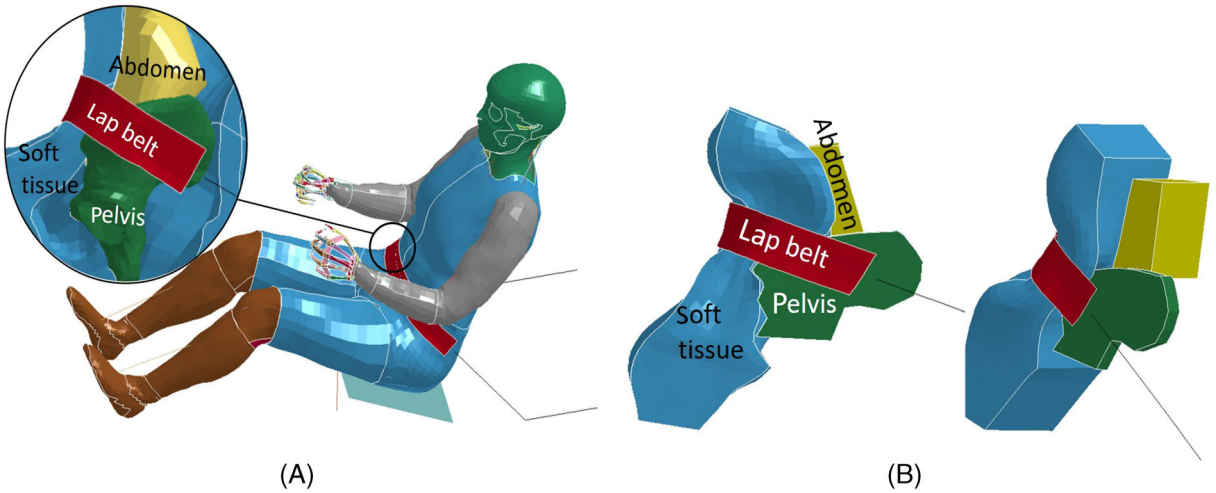

FIGURE 1 (A) The SAFER HBM v9 model used for inspiration for the submodel, and the details of the area of interest in the submarining study. (B) Modelling the area of interest through an FE pelvis submodel (two different perspectives)

This has also been confirmed through preliminary simulations where the boundary condition of soft tissue was altered without influencing the model response. Hexahedral elements incorporating full integration formulation (LS-DYNA solid element formulation 2) were used for the solid parts of the FE pelvis submodel. An approximate element size of 10 mm provides good convergent results where finer element sizes do not meaningfully influence the results. The skin, lap belt, and the cortical bone of the pelvis were meshed with shell elements. The verification of the FE pelvis submodel in capturing the lap belt-to-pelvis interaction can be found in previous work.[20]

2.2 | The constitutive model for adipose tissue

The material properties of adipose tissue are among parameters to be investigated in the lap belt-to-pelvis interaction. The previously developed material model[23] was used for adipose tissue and briefly introduced in this section. The rheological model is based on the generalised Maxwell viscoelastic model which consists of one elastic chain for equilibrium response (EQ) in parallel with N chains of Maxwell type (NEQ) for non-equilibrium behaviour. The model is designed to capture the response of a large span of strain rates. In the frame of finite strains, the model corresponds to the Reese and Govindjee[24] viscoelastic model in which the deformation gradient tensor $\mathbf{F}$ in the kth NEQ chain is multiplicatively split into an elastic part $\mathbf{F}_e^{(k)}$ and a viscous part $\mathbf{F}_v^{(k)}$. Correspondingly, the total strain energy is split into EQ and NEQ parts.

$$\mathbf{F} = \mathbf{F}_e^{(k)}\mathbf{F}_v^{(k)}, \quad k = 1,2,...,N \tag{1}$$

$$\Psi\left(\mathbf{F}, \mathbf{F}_v^{(1)}, \mathbf{F}_v^{(2)}..., F_v^{(N)}\right) = \Psi^{EQ} + \sum_{k=1}^{N} \Psi^{NEQ(k)}. \tag{2}$$

To better impose the incompressibility state of adipose tissue, the strain energy of each chain shall be further split into volumetric U and deviatoric $\widehat{\Psi}$ parts as

$$\begin{aligned}
&\Psi = \overbrace{\widehat{\Psi}^{EQ} + U^{EQ}}^{=\Psi^{EQ}} + \overbrace{\sum_{k=1}^{N}\left(\widehat{\Psi}^{NEQ(k)} + U^{NEQ(k)}\right)}^{=\Psi^{NEQ}} \\
&\widehat{\Psi}^{NEQ(k)} = A_v^{(k)}\left(\widehat{\mathrm{I}}_{C_e}^{(k)} - 3\right)^2, \quad \widehat{\Psi}^{EQ} = A_e(\mathrm{I}_C - 3)^2 \\
&U^{NEQ(k)} = \frac{\kappa_v^{(k)}}{2}\left(J^{(k)} - 1\right)^2, \quad U^{EQ} = \frac{\kappa_e}{2}(J-1)^2,
\end{aligned} \tag{3}$$

where $J = \det(\mathbf{F})$ and $J^{(k)} = \det(\mathbf{F}_e^{(k)})$ are the Jacobians of related deformation gradient tensors, $A_{\cdot}$ and $\kappa_{\cdot}$ are material parameters physically interpreted as the shear and bulk stiffness, receptively. According to previous work,[20] the linear term in the polynomials for $\widehat{\Psi}$ does not influence submarining response, thus, it is skipped here. Moreover, I_C and $\widehat{I}_{C_e}$ are the first invariants of $\mathbf{C}$ and $\widehat{\mathbf{C}}_e$. The evolution of viscous strain follows Reese and Govindjee[24] equation where, simply stated, an exponential relation between the viscous stress and the rate of viscous strain is defined. However, according to a previous study,[20] $\kappa_{\cdot}$ and $A_{\cdot}$ were the most important parameters which have been selected for this study. Therefore, for brevity, the details of the evolution of viscous strain have been omitted here, readers are referred to References 20,23 for further information.

The material model of adipose tissue used in this study consists of four viscoelastic chains in parallel with one elastic chain. Since the incompressibility condition is defined by Poisson's ratio, ν, the bulk modulus κ is replaced with ν via $\kappa = A[2(1+\nu)/3(1-2\nu)]$. The values of ν and $A^{(\cdot)}_{\text{nominal}}$ are given in Table 1.

2.3 | Belt-to-pelvis simulation

The schematic of lap belt-to-pelvis interaction is given in Figure 2 which defines belt angle, pelvis angle and initial lap belt position. The belt position is based on laboratory measurement of belt location for 54 men and women with different BMI in a previous study.[3] To account for obesity, only the thickness of subcutaneous adipose tissue was varied in the soft tissue between pelvis and lap belt. Four curves in Figure 2 represents the outer surface of soft tissue with different adipose tissue thickness. Comparing with belt position in previous studies,[3,4] these curves approximately correspond to the BMI of 25, 30, 35 and 40. The dots are midpoints of the belt and represent initial lap belt positions. The qualitative definition of submarining pertain to the lap belt suddenly slipping over the ASIS.[10,11,20] Typical submarining path and non-submarining path was shown in Figure 2. In lap belt-to-pelvis simulations, assigning the ASIS as the origin of coordinates for the midline belt position, the slide of belt over pelvis was unavoidable when the trajectory of the midpoint of the lap belt goes beyond $x > 25$ mm, Figure 2. Therefore, this was taken as the criteria to identify the belt slide in simulations.

Lap belt-to-pelvis parameters are divided into two categories: occupant parameters including adipose tissue material parameters (A,ν), pelvis angle, and the internal friction between the soft tissue and the pelvis (μ_{int}), and belt design parameters which are the external friction between the soft tissue and lap belt (μ_{ext}), belt pulling rate, belt force, and belt angle. The belt angle has been defined as the angle between the lap belt and the horizontal line in the sagittal (xz) plane. The pelvic angle follows the definition in Reference 25 which is the line through the midpoint of the sacral plate and midpoint of the femoral heads axis, and the vertical line. The centres of rotation for the pelvis angle and the belt angle are the ASIS and the midpoint belt, respectively. Three levels for each parameter have been assumed, represented by parameter sets of $\mathbf{X}_1$, $\mathbf{X}_2$, and $\mathbf{X}_3$ in Table 2 where the nominal values are collected in $\mathbf{X}_2$. For example, in seated position with nominal seat back angle, the average pelvis angle measured 32° in a previous study[26] which was selected as the nominal value with ±6° standard deviations for the other two levels. For the coefficient friction between the soft tissue and the pelvis μ_{int}, although no study was found, it is 0.2 in the SAFER HBM v9 which has been defined as the nominal value. Values for the belt rate, belt force, and the belt angle are based on the expected values during a typical vehicular crash. Similar levels can be found in other studies.[11,12] The values in Table 1 have been selected as the nominal values of the material parameters of adipose tissue (A,ν). The other two levels of A and ν have been estimated based on the variation of adipose tissue behaviour in an indentation test[27] and a frequency sweep test.[28]

The three levels for each parameter have been ordered such that from $\mathbf{X}_3$ to $\mathbf{X}_1$ it is more likely to have belt sliding over the pelvis. For example, a higher level of belt force in $\mathbf{X}_1$ increases the risk for the belt sliding. Through preliminary simulations, a region in front of ASIS where the result of belt-to-pelvis interaction depends on the parameters given in Table 2 was identified. This region is between the lines $\mathbf{X}_1$ and $\mathbf{X}_3$ in Figure 2. Hence, regardless of parameter values, the slide of the belt does not occur anterior-inferior to the line $\mathbf{X}_1$ while superior-posterior to the line $\mathbf{X}_3$ it is

TABLE 1 The material parameters for adipose tissue[23]

	EQ	NEQ (1)	NEQ (2)	NEQ (3)	NEQ (4)
$A^{(\cdot)}_{nominal}$	0.2 kPa	0.4 kPa	0.83 kPa	1.63 kPa	4 kPa
ν	0.4995	0.4995	0.4995	0.4995	0.4995

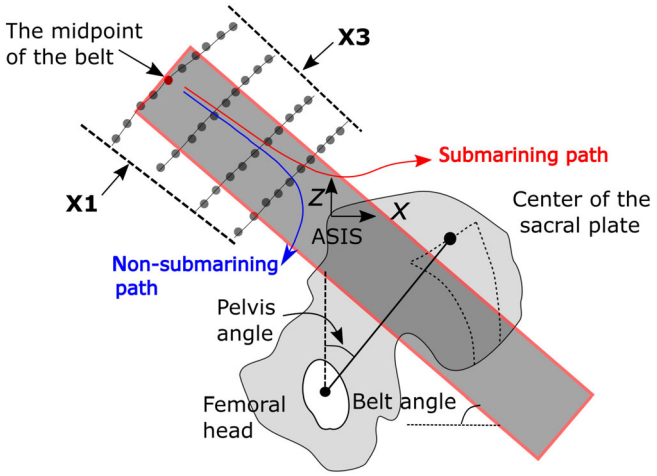

FIGURE 2 The four curves represent the outer surface of soft tissue with different thickness of subcutaneous adipose layers. The dots on the curves represent the possible initial lap belt positions based on a previous study on belt location for 54 subjects with different BMI.[3] The pelvic angle, as defined in Reference 25, is the line through the midpoint of the sacral plate and midpoint of the femoral heads axis, and the vertical. The belt angle is the angle between the lap belt and the horizontal in the sagittal (XZ) plane

TABLE 2 Different levels of belt design and occupant related parameters

	Belt parameters				Occupant parameters			
Level	**Belt angle**	μ_{ext}	**Pulling rate**	**Belt force**	**Pelvis angle**	μ_{int}	$A^{(\cdot)}$	ν
$\mathbf{X}_1$	30°	0.1	7 m/s	6 kN	38°	0.05	$0.5\,A^{(\cdot)}_{\text{nominal}}$	0.49500
$\mathbf{X}_2$	45°	0.3	4 m/s	3 kN	32°	0.20	$1.0\,A^{(\cdot)}_{\text{nominal}}$	0.49950
$\mathbf{X}_3$	60°	0.6	1 m/s	1 kN	26°	0.40	$2.0\,A^{(\cdot)}_{\text{nominal}}$	0.49995

unavoidable. To investigate belt-to-pelvis interaction between the line $\mathbf{X}_1$ and $\mathbf{X}_3$, each curve has been discretised by 10 roughly equidistant points.

2.4 | Individual parameter study

To separately evaluate the influence of each parameter, one parameter varied at the time to either its $\mathbf{X}_1$ or $\mathbf{X}_3$ value while other parameters have their nominal values, $\mathbf{X}_2$. Hence, two model evaluations for each parameter were required. In addition, the model was evaluated for the nominal values of $\mathbf{X}_2$. In total, $[8\,(\text{parameters}) * 2\,(\text{variations}) + 1\,(\text{nominal behavior})] * 40\,(\text{points}) = 680$ model evaluations were conducted in this step. For each such case, the simulation result has been categorised either as *slide* or *no slide*.

2.5 | The full variation

Two belt design parameters and two occupant parameters are selected from the previous step as influential parameters. The aim was to estimate the risk of belt slide for different selections of design parameters as a function of occupant parameters. Belt design parameters creates a 2×2 matrix of different belt design selections. For each selection, all variation of occupant parameters were evaluated. So, $4\,(\text{Belt design selections}) * 2^2(\text{Occupant parameter variations}) * 40\,(\text{points}) = 640$ model evaluations were performed in this step. Finally, the risk of belt slide has been estimated by assuming equal weights for each level of occupant parameter.

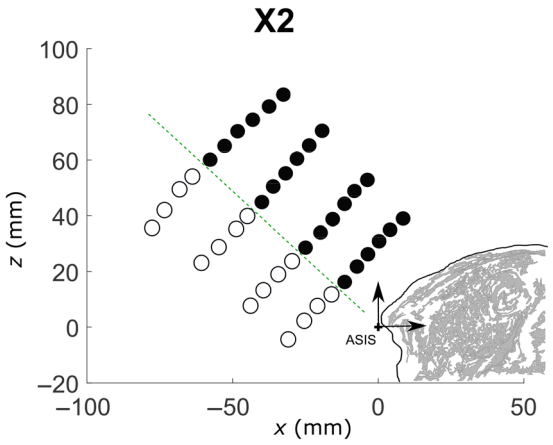

FIGURE 3 The evaluation of nominal values in the parameter-dependent region; white circles: *no slide*, black circles: *slide*

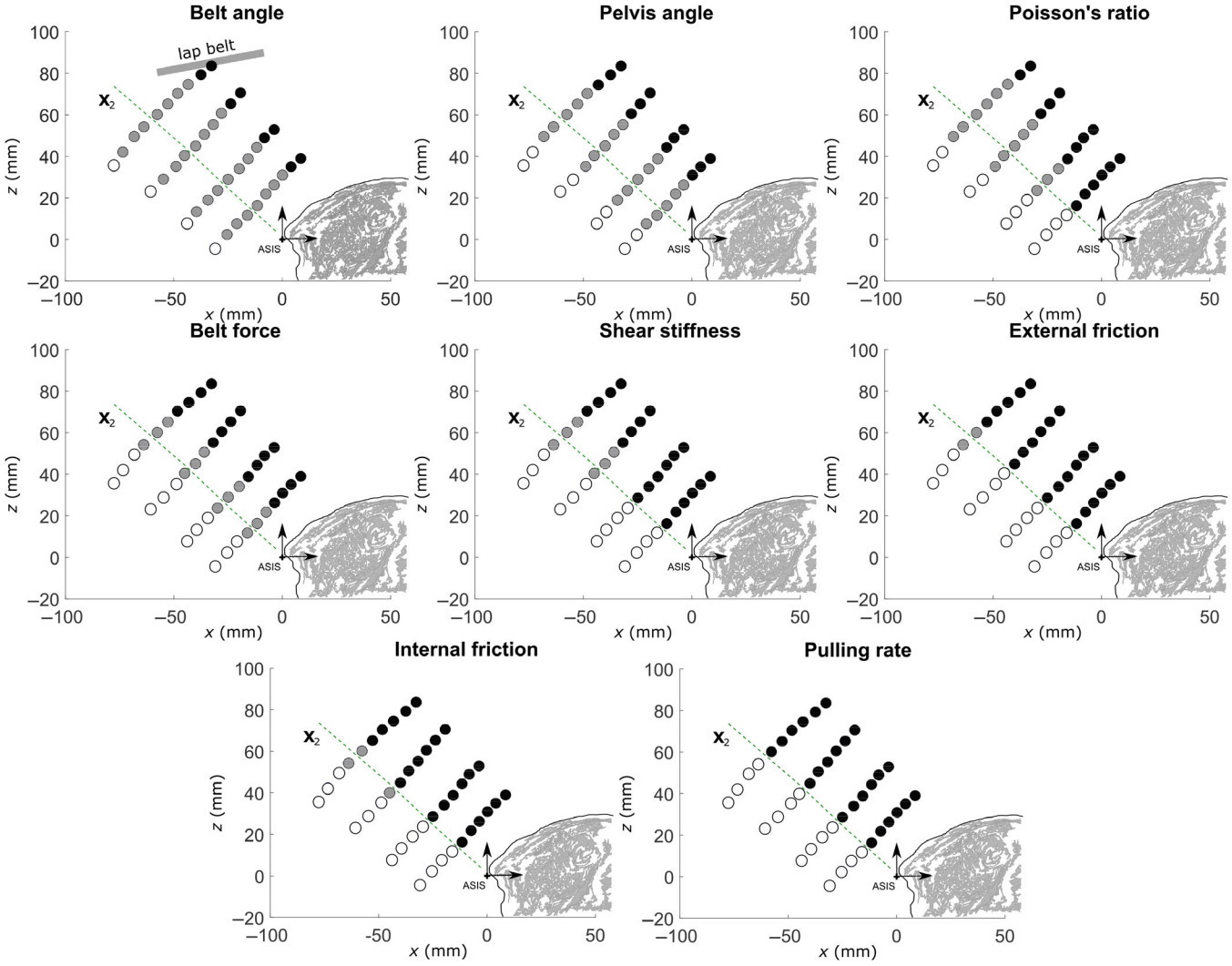

FIGURE 4 The influence of individual parameter on the belt slide where two parameter variation were evaluated. White circles: *no slide*, black circle: *slide*, grey circles: one *slide*, one *no slide*

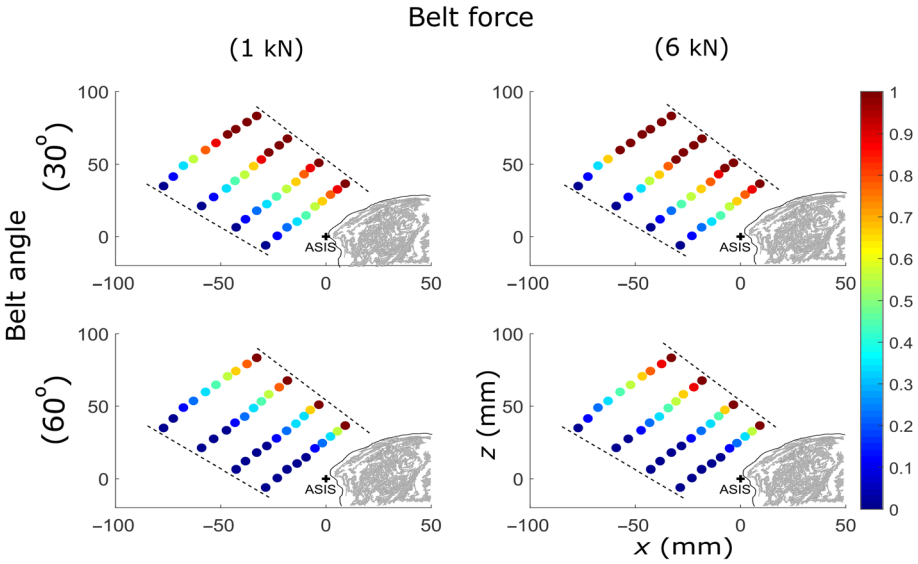

FIGURE 5 The estimated risk of belt slide for different selections of belt design parameters. Red indicates high risk for belt slide and blue is for low risk

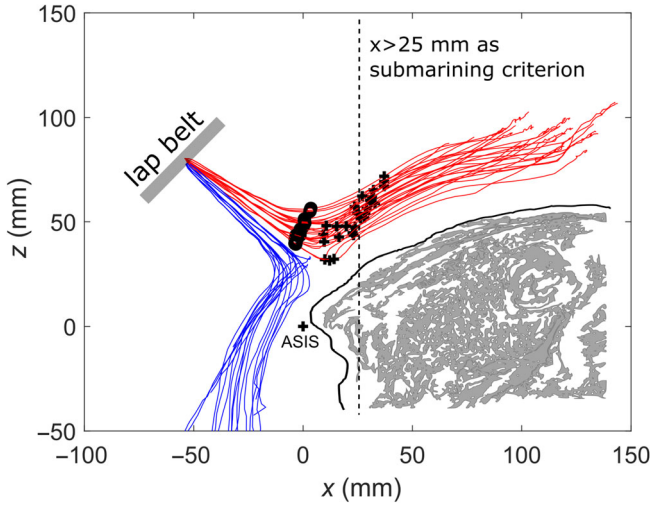

FIGURE 6 All belt trajectories starting from one point; for submarined cases, the two time frames of 26 and 40 ms are marked with (o) and (+), respectively

3 | RESULTS

3.1 | Individual parameter study

First, nominal behaviour was evaluated for each point, Figure 3. The result either indicates *no slide* or *slide* shown by a white circle or a black circle, respectively, separated by a green dashed line. Then, variation of each parameter to either $\mathbf{X}_1$ or $\mathbf{X}_3$ were evaluated at each point. If both variations result in *no slide* it is indicated by a white circle. If both variations result in *slide* the point is represented by a black circle. Finally, if one variation results in *slide* and the other one is *no slide* it is shown by a grey circle. Thus, the more grey circles the more influential is the parameter for the slide/no slide outcome. The results for each parameter are shown in Figure 4. The belt angle, belt force, pelvis angle, and Poisson's ratio appear to be the most important parameters identified in this step.

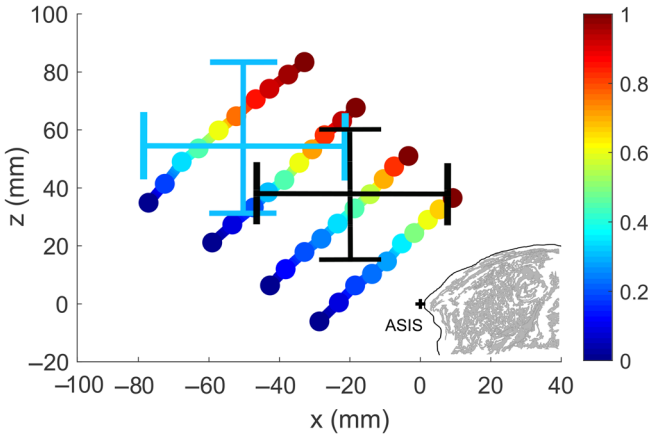

FIGURE 7 The estimated risk of belt slide for different belt positions in front of ASIS was compared with plus or minus one standard deviation of belt position in a laboratory study.[3] Black bars are for obesity group with BMI < 30 and blue bars are for obesity group with BMI > 30

3.2 | The full variation

The important parameters identified from the primary effect simulation, that is, the belt angle, belt force, pelvis angle, and Poisson's ratio, were used for further studies. The two plus two design levels, 60° and 30°, for the belt angle and 6 and 1 kN for the belt force, provides four belt design selections. For each selection, the effect of full variation of pelvis angle and Poisson's ratio was evaluated, Figure 5.

4 | DISCUSSION

Simulations where the trajectory of the midpoint belt exceeded $x > 25$ mm have been identified as *slide* cases. The reason for selecting 25 mm is that it is half of the width of a typical belt, that is, the midpoint, and passing the midpoint of the lap belt from $x = 25$ mm means the whole belt will have slipped over the ASIS. Hence, submarining would probably be unavoidable. Moreover, to ensure that it is correctly identified using this criterion, all belt trajectories starting from one initial point were plotted in one figure and the accuracy of submarining identification has been visually confirmed. Figure 6 is one example of such a figure. As it can be seen, the belt trajectories of all submarining cases with the $x > 25$ mm criterion have been plotted in red whereby the correct submarining identification can be simply confirmed. To better understand lap belt-to-pelvis interaction, it is worth looking closer at the belt trajectory. Two specific time frames of 26 and 40 ms have been marked for the belt sliding cases. These occur approximately the instance before and after the belt slide. As belt trajectory is more superior to the ASIS, its path between the two occurrences becomes longer indicating a weaker engagement of the lap belt to the ASIS.

Outside the region between the lines of $\mathbf{X}_1$ and $\mathbf{X}_3$ the outcome is certain, regardless of parameter values in Table 2. Hence, parameters have only been studied between $\mathbf{X}_1$ and $\mathbf{X}_3$. First, the influence of one parameter change at the time was studied to initially filter out the non-sensitive parameters, then, further extensive analysis was conducted to account for the interaction between the identified sensitive parameters, and to understand how belt position and soft tissue thickness can influence the risk of belt slide. The influence of each parameter is separately compared with the nominal behaviour. The number of grey circles for each parameter shows the consequent deviation from the nominal behaviour, thus, it might be interpreted as the parameter effect on the belt slide. Hence, the belt angle has been identified as the most influencing parameter among all parameters, since it has more grey circles than any other. Further design parameters that has major effect includes belt force. Among the occupant parameters, the pelvis angle and Poisson's ratio of adipose tissue has been identified as important parameters. Poisson's ratio has also been identified as an influential parameter in previous work[20,29] where impact behaviour of adipose tissue was studied. Generally, more grey circles are present at thicker layers of the soft tissue in front of the ASIS, for example, for Poisson's ratio, the shear stiffness and the friction. This indicates that the influence of these parameters extend with obesity. The pulling rate parameter showed the least effect as it represents the same results as the nominal values.

The risk of belt slide for the space in front of the ASIS has been quantified by a number between 0 and 1, Figure 5. In general, the further away (or superior-posterior) to the ASIS the initial lap belt position is, the more likely the risk of belt slide will be. This implies that for a thicker soft tissue layer, the joint effects of parameters are synergistically accumulating, resulting in a higher risk of submarining. The belt slide risk is only marginally influenced by the belt force. However, the belt angle can substantially change this risk. A low belt angle at 30° substantially increases the risk such that belt slide is almost unavoidable in the superior-posterior part where the red colour is dominant. On the other side, the belt angle of 60° secures the hooking between the belt and the pelvis, subsequently reducing the risk of belt slide substantially.

The effect of muscle tissue thickness was not considered and obesity was attributed to an increase in the thickness of subcutaneous adipose tissue. This assumption was supported in a study on measurement of abdominal muscle and subcutaneous fat thickness.[19] It was found that, regardless of age and gender, subcutaneous adipose tissue thickness significantly correlated with waist circumference, but muscle tissue thickness did not. Moreover, ageing was always associated with a reduce in muscle thickness and an increase of subcutaneous adipose tissue. Therefore, the predicted higher risk of belt slide with thicker adipose layer also indicates a higher risk of belt slide with obesity. For example, the estimated risk of belt slide in this study was compared with belt location of 54 subjects with BMI > 30 (as obese) and BMI < 30 (as non-obese),[3] Figure 7. As it is shown, obese occupants are in general at higher risk for the lap belt to slid over pelvis. In a previous study on the effect of obesity on lap belt path,[8] obesity was associated with a lower belt angle and more forward belt position relative to the pelvis. According to Figure 5, the low belt angle will exacerbate the risk of belt slide for obese occupants.

There are some limitations to this study. Firstly, all parameters have been assumed independent although different parameters may correlate. For example, in a previous study,[3] a correlation between the lap belt position with the belt angle and BMI has been given. That might be partly because the lap belt anchorage points are fixed for a given seat setting while in this study the lap belt rotates around the midpoint belt. Subsequently the belt anchorage moves, thus, the belt angle becomes independent of the initial lap belt position. Therefore, it is likely that the probability for different points in front of the ASIS are different to the belt angle. However, the aim of this study is not to provide the submarining risk as expected in real vehicle crashes to develop corresponding safety countermeasures. Instead it aims to identify the most important parameters among many parameters, as well as to illustrate how the interaction between parameters may affect lap belt-to-pelvis interaction. The results of the present study are suitable for the development of FEHBMs and designing tests for further study of submarining. Different sitting configurations may alter the parameter ranges studied here. For example, seat back angle can influence lumbar spine alignment which affects pelvis angle, belt angle and belt positions. Parameter variation covered here (pelvis angle, seat belt angle) and initial belt positions are based on nominal seating configuration, with a seat back angle around to 23°–25°, and nominal spine alignment from literature. So, the results in the present study apply to a nominal seating configuration. In future autonomous vehicles more relaxed sitting positions are expected which may bring different lumbar spine alignment. This will bring quite different parameter variation and belt-to-pelvis interaction which is left for future studies. Another limitation includes lap belt-to-pelvis interaction was studied in a static state, that is, the human body (or the pelvis) was assumed fixed when the lap belt is pulled similar to tests previous studies.[10–12,30] In a real crash, on the other hand, the human body is not fixed. During a crash, the kinetic energy of the occupant will make the occupant move relative to the seat until being stopped by the seat belt. A thick layer of soft tissue will provide slack in the hooking. The negative effect of the slack becomes even more critical when the pelvis moves and slides under the belt due to the relative motion. A possible rotation of the pelvis, as well as some downwards pelvis motion occurring as the lap belt loads the pelvis downward, can also increase the risk of submarining.

5 | CONCLUSION

The effect of different belt design and occupant parameters on lap belt-to-pelvis interaction has been investigated. It is found that the lap belt angle represents the most influential design parameter. Important occupant parameters include the pelvis angle and the Poisson's ratio of the adipose tissue. With obesity and a thicker layer of soft tissue, the interaction effects between these parameters are synergistically accumulated resulting in an increased risk of belt slide over the pelvis.

ACKNOWLEDGEMENTS

This work has received funding from Swedish Research Council (VR), Grant No. 621-2013-3909, and the European Union's Horizon 2020 research and innovation program (the OSCCAR project), Grant No. 768947, which are gratefully acknowledged.

CONFLICT OF INTEREST

The authors declare no conflicts of interest.

DATA AVAILABILITY STATEMENT

Data sharing not applicable to this article as no datasets were generated or analysed during the current study.

ORCID

Hosein Naseri https://orcid.org/0000-0002-8577-4739
Johan Iraeus https://orcid.org/0000-0001-9360-0707
Håkan Johansson https://orcid.org/0000-0002-7207-8486

REFERENCES

1. Grime G. A review of research on the protection afforded to occupants of cars by seat belts which provide upper torso restraint. *Accid Anal Prev*. 1979;11(4):293-306. doi:10.1016/0001-4575(79)90055-1
2. Adomeit D, Heger A. *Motion Sequence Criteria and Design Proposals for Restraint Devices in Order to Avoid Unfavorable Biomechanic Conditions and Submarining*. SAE International; 1975.
3. Reed MP, Ebert-Hamilton SM, Rupp JD. Effects of obesity on seat belt fit. *Traffic Inj Prev*. 2012;13(4):364-372.
4. Reed MP, Ebert SM, Hallman JJ. Effects of driver characteristics on seat belt fit. *Stapp Car Crash J*. 2013;57:43-57.
5. Forman J, Lopez-Valdes FJ, Lessley D, Kindig M, Kent R, Bostrom O. The effect of obesity on the restraint of automobile occupants. *Ann Adv Automot Med*. 2009;53:25-40.
6. Shi X, Cao L, Reed MP, Rupp JD, Hu J. Effects of obesity on occupant responses in frontal crashes: a simulation analysis using human body models. *Comput Methods Biomech Biomed Engin*. 2015;18(12):1280-1292.
7. Turkovich M, Hu J, van Roosmalen L, Brienza D. Computer simulations of obesity effects on occupant injury in frontal impacts. *Int J Crashworthiness*. 2013;18(5):502-515. doi:10.1080/13588265.2013.809646
8. Jones ML, Ebert S, Hu J, Reed MP. *Effects of High Levels of Obesity on Lap and Shoulder Belt Paths*. International Research Council on Biomechanics of Injury (IRCOBI); 2017:13-15.
9. Hartka TR, Carr HM, Smith BR, Melmer M, Sochor MR. Does obesity affect the position of seat belt loading in occupants involved in real-world motor vehicle collisions? *Traffic Inj Prev*. 2018;19(sup1):S70-S75.
10. Uriot J, Baudrit P, Potier P, et al. Investigations on the belt-to-pelvis interaction in case of submarining. *Stapp Car Crash J*. 2006;50:53-73.
11. Kim T, Park G, Montesinos S, et al. Abdominal characterization test under lap belt loading. Paper presented at: 24th International Technical Conference on the Enhanced Safety of Vehicles (ESV); 2015; Gothenburg, Sweden:National Highway Traffic Safety Administration.
12. Luet C, Trosseille X, Drazétic P, Potier P, Vallancien G. Kinematics and dynamics of the pelvis in the process of submarining using PMHS sled tests. *Stapp Car Crash J*. 2012;56:411-442.
13. Gayzik FS, Moreno DP, Vavalle NA, Rhyne AC, Stitzel JD. Development of the global human body models consortium mid-sized male full body model. Paper presented at: Proceedings of the 39th International Workshop on Human Subjects for Biomechanical Research; 2011: National Highway Traffic Safety Administration.
14. Iwamoto M, Kisanuki Y, Watanabe I, Furusu K, Miki K, Hasegawa J. Development of a finite element model of the total human model for safety (THUMS) and application to injury reconstruction. Paper presented at: Proceedings of the 2002 International Research Council on Biomechanics of Injury; 2002; Munich, Germany:31–42.
15. Iwamoto M, Nakahira Y, Kimpara H. Development and validation of the Total HUman Model for Safety (THUMS) toward further understanding of occupant injury mechanisms in precrash and during crash. *Traffic Inj Prev*. 2015;16(sup1):S36-S48. doi:10.1080/15389588.2015.1015000
16. Gepner BD, Joodaki H, Sun Z, et al. Performance of the obese GHBMC models in the sled and belt pull test conditions. Paper presented at: Proceeding of the International Research Council on the Biomechanics of Injury (IRCOBI) (IRC-18-60); 2018; Athens, Greece.
17. Foster CD, Hardy WN, Yang KH, King AI, Hashimoto S. High-speed seatbelt pretensioner loading of the abdomen. *Stapp Car Crash J*. 2006;50:27-51.
18. Cavanaugh JM, Nyquist GW, Goldberg SJ, King AI. Lower Abdominal Tolerance and Response. SAE Technical Paper 861878; 1986.
19. Kanehisa H, Miyatani M, Azuma K, Kuno S, Fukunaga T. Influences of age and sex on abdominal muscle and subcutaneous fat thickness. *Eur J Appl Physiol*. 2004;91(5):534-537.
20. Naseri H, Iraeus J, Johansson H. The effect of adipose tissue material properties on the lap belt-pelvis interaction: a global sensitivity analysis. *J Mech Behav Biomed Mater*. 2020;107:103739. doi:10.1016/j.jmbbm.2020.103739
21. Iraeus J, Pipkorn B. Development and validation of a generic finite element ribcage to be used for strain-based fracture prediction. Paper presented at: Proceedings of the 2019 International Research Council on Biomechanics of Injury; 2019; Florence, Italy:193–210.
22. Pipkorn B, Iraeus J, Björklund M, Bunketorp O, Jakobsson L. Multi-scale validation of a rib fracture prediction method for human body models. Paper presented at: Proceedings of the 2019 International Research Council on Biomechanics of Injury; 2019; Florence, Italy:175–192.

23. Naseri H, Johansson H, Brolin K. A nonlinear viscoelastic model for adipose tissue representing tissue response at a wide range of strain rates and high strain levels. *J Biomech Eng*. 2018;140(4):041009.
24. Reese S, Govindjee S. A theory of finite viscoelasticity and numerical aspects. *Int J Solids Struct*. 1998;35(26-27):3455-3482.
25. Boulay C, Tardieu C, Hecquet J, et al. Sagittal alignment of spine and pelvis regulated by pelvic incidence: standard values and prediction of lordosis. *Eur Spine J*. 2006;15(4):415-422. doi:10.1007/s00586-005-0984-5
26. Beillas P, Lafon Y, Smith FW. *The Effects of Posture and Subject-to-Subject Variations on the Position, Shape and Volume of Abdominal and Thoracic Organs*. The Stapp Association; 2009.
27. Gefen A, Haberman E. Viscoelastic properties of ovine adipose tissue covering the gluteus muscles. *J Biomech Eng*. 2007;129(6):924-930.
28. Geerligs M, Peters GW, Ackermans PA, Oomens CW, Baaijens F. Linear viscoelastic behavior of subcutaneous adipose tissue. *Biorheology*. 2008;45(6):677-688.
29. Naseri H, Johansson H. A priori assessment of adipose tissue mechanical testing by global sensitivity analysis. *J Biomech Eng*. 2018; 140(5):051008.
30. Steffan H, Hofinger M, Parenteau C, et al. Abdominal responses to dynamically lap belt loading. Paper presented at: Proceedings of the IRCOBI Conference; 2002. Munich, Germany. p. 315.

How to cite this article: Naseri H, Iraeus J, Johansson H. A numerical study on the safety belt-to-pelvis interaction. *Int J Numer Meth Biomed Engng*. 2022;38(4):e3572. doi:10.1002/cnm.3572